# Wide-Angle X-ray Scattering, Fourier Transform Infrared Spectroscopy, and Scanning Electron Microscopy Studies on the Influence of the Addition of Liquid Functional Rubber into Epoxy Thermoset

**VINEETA NIGAM, D. K. SETUA, G. N. MATHUR**

Defence Materials and Stores, Research & Development Establishment, G. T. Road, Kanpur-208 013, India

*Received 17 November 1997; accepted 22 February 1998*

**ABSTRACT:** Sophisticated analytical methods (viz. wide-angle X-ray scattering, Fourier transform infrared spectroscopy, and scanning electron microscopy have been applied to investigate the mechanism of toughening of epoxy cresol novolac resin due to the addition of carboxy-terminated polybutadiene (CTPB) liquid functional rubber. The average molecular interchain spacing $\langle R \rangle$ in Angstroms of neat epoxy and epoxy–rubber blends were calculated from the strong maximum in the diffraction scan using established equations. The half-width $\langle HW \rangle$ of the maximum was used to qualitatively describe the distribution of $\langle R \rangle$. An increase in $\langle R \rangle$ value signifies formation of a separate packing order, as well as an increase in the free volume which, however, varies with the extent of compatibilization between epoxy cresol novolac and CTPB. Fourier transform infrared studies convincingly establish the crosslinking between the oxirane group of epoxy and the carboxyl group of CTPB as reflected in the characteristic peak shifts in the blends, compared with individual polymers. The merger of several peaks of individual polymers, as well as the appearance of minor peaks elsewhere, were also evident. Scanning electron microscopy studies have also been undertaken to study the phase morphology development, as well as changes in the fracture surface topography with varied CTPB content. © 1998 John Wiley & Sons, Inc. J Appl Polym Sci 70: 537–543, 1998

**Key words:** epoxy cresol novolac; carboxy-terminated polybutadiene; toughening; infrared spectroscopy; wide-angle X-ray scattering

## INTRODUCTION

Epoxy resins are frequently toughened by the addition of rubber particles and as such these blends find extensive usage as structural adhesives and matrices for fiber and particulate composites.[1–15] The toughness characteristics of epoxy thermosets have been studied in the past, and this subject still remains a matter of great debate concerning the paramount factors governing fracture, deformation, and ultimate ductility.[16,17] Studies have been made by Pearson and Yee[3,4,18,19] on elastomer-modified epoxies with respect to their mechanical properties, crosslink density, and mechanism of toughening, as well as scanning electron microscopy (SEM) depicting the phase morphology of the fractured surface of rubber-modified epoxies. Evaluation of effective crosslink density of matrix resin, measurement of glass transition temperature and cure characterization through differential scanning calorimetry and dynamic mechanical analysis of diglycidyl ether of bisphenol-A (DGEBA) modified with carboxy-terminated copolymer of butadiene acryloni-

*Correspondence to:* D. K. Setua.

Journal of Applied Polymer Science, Vol. 70, 537–543 (1998)
 CCC 0021-8995/98/030537-07

trile (CTBN) has also been reported.[18,20] Qian and colleagues[21] studied the synthesis and application of core-shell particles as toughening agents for epoxies. Bagheri and Pearson[22] have studied the interfacial phenomenon of CTBN-modified epoxies. Chen and Jan[23] have extensively studied the effect of matrix ductility on the fracture behavior of rubber-toughened epoxy resins. Kinloch and Hunston[24] studied the effect of volume fraction of dispersed rubbery phase (CTBN) on the toughness of epoxy (DGEBA) polymers. We have only recently reported our studies on cure characteristics, dynamic mechanical properties, and phase morphology development of epoxy cresol novolac (ECN)–carboxy-terminated polybutadiene (CTPB) blends.[25,26]

A particular wavelength of X-ray when impinging upon a polymer gets scattered. Extent of this scattering is dependent on the molecular order within the polymer. Wide-angle X-ray scattering (WAXS) of crystalline polymers consists of sharp lines or peaks that indicate distinct interatomic distances between highly ordered planes. The WAXS diffractogram for a semicrystalline polymer has the X-ray scattering intensity spread due to less ordered crystalline planes and the amorphous scatter. Thus, molecular disorders, configuration, or spatial arrangement of bonds can be measured by WAXS.[27] Kunz and colleagues[28] have determined the volume fraction and interface width using X-ray analysis of the dispersed rubber particle–matrix interfacial region for an amine-cured rubber-modified epoxy. Diffused appearance of an amine-terminated copolymer of butadiene acrylonitrile (ATBN)-modified epoxy was attributed to irregularly shaped particles, in comparison with more spherical-shaped particles for CTBN-modified epoxy. Wang and Zupko[29] gave evidence for the completion of phase separation at the point of gelation, but showed that compositional changes continued to take place. Gillham and Chan[30] used a light transmission method to study phase separation behavior and found a higher volume fraction of phase-separated rubber for ATBN-modified epoxy, compared with CTBN-modified epoxy.

Verchere and colleagues[31] showed shear deformation of the matrix as major toughening mechanism. Moschiar and coworkers[32] studied the phase separation model for analysis of epoxy-terminated copolymer of butadiene acrylonitrile-modified diepoxide (DGEBA) and diaminodiphenyl methane (DDM). Bagheri and Pearson[33] studied the role of blend morphology in rubber-toughened polymers. Kim and coworkers[34] reported the effect of particle size and rubber content on fracture toughness of DGEBA by core-shell rubber particles. In this article, an attempt has been made to investigate the molecular disorder in epoxy network in the liquid rubber-toughened epoxy system by the WAXS technique. The effect of different percentage of liquid rubber on the characteristic value of $\langle R \rangle$ (interchain spacing) and $\langle HW \rangle$ (half-width) have been determined. The crystallinity index (CI) of blend systems has also been calculated, as described by Halasa and colleagues.[27] Compositional changes of the blends associated with the addition of CTPB and its efficacy of crosslinking and functionality changes by Fourier transform infrared (FTIR) spectroscopy have also been studied. Studies also include the mechanically flex fractured surface morphology of the blends to interpret the microstructural changes and failure mechanism in relation to increasing CTPB concentration.

**Table I Characteristic Properties of CTPB**

| Property | Values |
|---|---|
| Brookfield viscosity [MPa s (27°C)] | 60000 |
| Carboxyl content (%) | 1.9 |
| Specific gravity (25°C) | 0.907 |
| % volatiles | <2.0 |
| Functionality | 2 |

## EXPERIMENTAL

### Blends Preparation

Table I shows the characteristic properties of CTPB (Hycar CT-RLP, 2000 × 162) used in the present study.

Table II shows the formulation of the mixes with varied ECN and CTPB contents, along with the requisite amount of DDM used as a curing agent for epoxy. The weight of DDM was affixed on the epoxide equivalent weight (ASTM D-1652) of the ECN. To a preheated and mechanically stirred epoxy novolac resin, CTPB followed by DDM were mixed at 60–70°C until complete dissolution. The blends were then moulded into sheets in a pretreated iron mold at 140–145°C and postcured at 200°C for 2 h each.

FTIR experiments were conducted on a Nicolet Magna 750 infrared spectrometer using KBr pel-

**Table II Composition of ECN and CTPB Blends Containing DDM**

| Blend No.[a] | ECN | CTPB | DDM |
|---|---|---|---|
| $ERB_0$ | 100 | 0 | 23.0 |
| $ERB_5$ | 95 | 5 | 21.5 |
| $ERB_{10}$ | 90 | 10 | 20.0 |
| $ERB_{15}$ | 85 | 15 | 19.2 |
| $ERB_{25}$ | 75 | 25 | 17.1 |

[a] ERB indicates epoxy–rubber blend; subscript indicates percent of rubber content.

lets. X-ray studies were performed on 250 × 125 × 4 mm thick samples prepared by a diamond edge cutter. Wide-angle X-ray equatorial scans of the cured blends were made at room temperature (25 ± 2°C) using a Philips X-ray powder diffractometer APD 15; CuK$\alpha_1$ radiation ($\lambda$ = 1.5418 Å). Measurements were done in reflection mode using the XRD parameters [Nickel filter, 45 kV, 25 mÅ, step scan: 6–40° (2$\theta$), step size: 0–2°, and counting time: 10 s]. The intensity counts collected were corrected for polarization and absorption. Corrections were also made in respect to air scatter. The corrected intensity was smoothed and plotted versus the angle of diffraction (2$\theta$). The position of the "peak maximum" was computed from the Bragg's diffraction equation:

$$n\lambda = 2d \text{ Sin } \theta \rightarrow \quad (1)$$

where $n$ is order of reflection, $\lambda$ is wavelength of radiation, $d$ is interplanar distance, and 2$\theta$ is angle of diffraction. The average interchain separation, $\langle R \rangle$ in Angstroms, that gives rise to the strong maximum in the equatorial scan was calculated from the following equation:

$$\langle R \rangle = 5/8\ (\lambda/\text{Sin } \theta) \rightarrow \quad (2)$$

The half-width $\langle HW \rangle$ of the WAXS amorphous maximum is the qualitative expression of the distribution of $\langle R \rangle$ and was calculated from the diffraction plot of 2$\theta$ versus intensity. Using the Bragg's equation, the "$d$" spacings were determined for the strong maximum at half-height intensity. The half-width is the difference between these two calculated "$d$" spacings. An example of the calculation for $\langle R \rangle$ and $\langle HW \rangle$ for an amorphous system is shown in Figure 1.

SEM studies were conducted in a JEOL JSM 35 CF scanning electron microscope. The fractured surfaces obtained from flex failed test specimens were sputter-coated with gold without touching the surface and stored in a dessicator for SEM observations. Details of sample preparation and recording of SEM photographs have been mentioned elsewhere.[35]

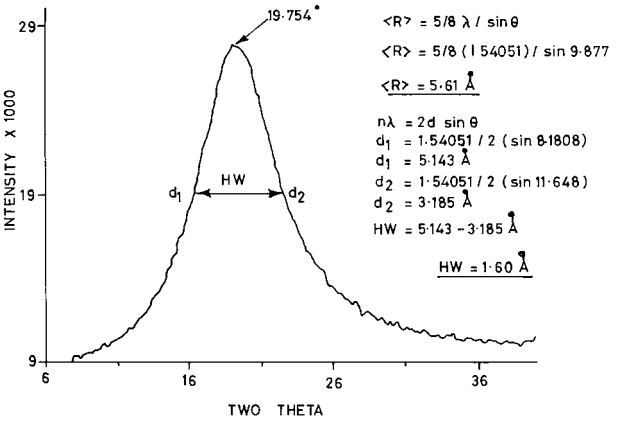


**Figure 1** Calculation of $\langle R \rangle$ and $\langle HW \rangle$ for an amorphous system.

## RESULTS AND DISCUSSIONS

The WAXS studies of neat epoxy and the ECN-CTPB blends showed a steady increase of $\langle HW \rangle$ with increasing rubber concentration up to 15 wt %, beyond which $\langle HW \rangle$ increases abruptly. Interchain spacing $\langle R \rangle$ also shows a similar trend as the CTPB concentration in the blends is increased. Results are tabulated in Table III. From 5 to 15 wt % CTPB, the blends show a slow increase in $\langle R \rangle$, which is then followed by a sharp rise in case of 25 wt % rubber. Nature of changes in the $\langle HW \rangle$ and $\langle R \rangle$ values thus signifies the development of a new molecular structure and

**Table III Interchain Spacing, Half-Width, and "*d*" Spacing for Blend Systems**

| Blend No.[a] | "$d$" (Å) | $\langle R \rangle$ (Å) | $\langle HW \rangle$ (Å) |
|---|---|---|---|
| $ERB_0$ | 4.61 | 5.76 | 2.46 |
| $ERB_5$ | 4.63 | 5.85 | 2.56 |
| $ERB_{10}$ | 4.64 | 5.86 | 2.62 |
| $ERB_{15}$ | 4.65 | 5.88 | 2.68 |
| $ERB_{25}$ | 4.68 | 5.92 | 3.32 |

[a] ERB indicates epoxy–rubber blend; subscript indicates percent of rubber content.

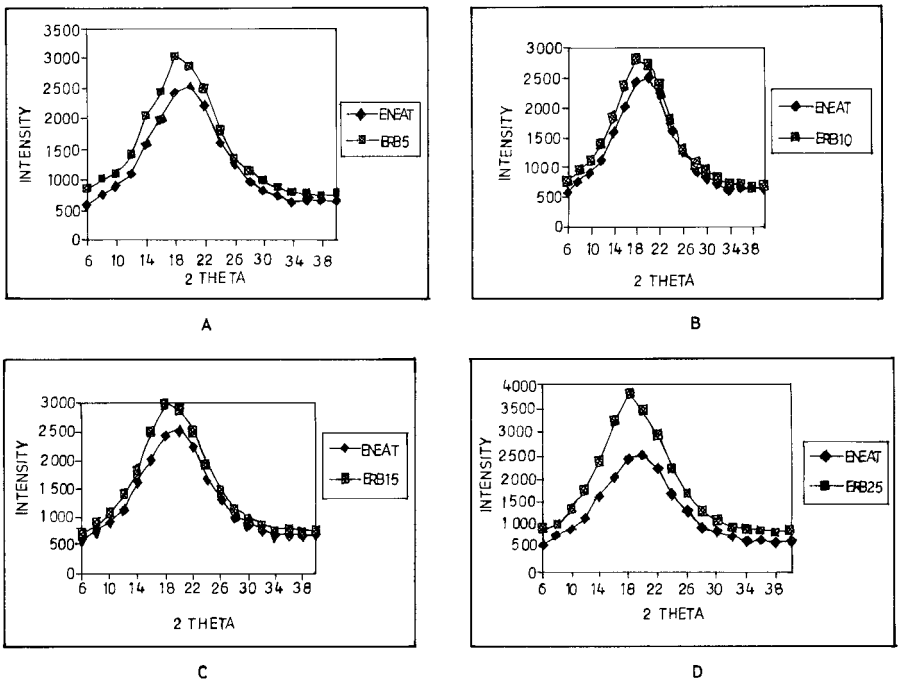


**Figure 2** WAXS diffractograms of different epoxy–rubber blends, each plotted against neat epoxy.

stretching of the molecular chains further apart, resulting in an increase of interchain spacing.

CI is defined as the degree of ordering in systems. CI can be calculated as the ratio of the crystalline to the total peak area.[23] The traditional concept of crystalline and amorphous regions in polymers has undergone a rational transformation in recent years. In the case of ECN–CTPB blends, miscibility values were obtained by calculating the crystallinity of the systems from WAXS profile data. Figure 2 shows the WAXS profiles for all of the blend systems and, in each case, a blend is compared with that of the neat resin. CI of the blends are shown in Figure 3. CI increases as the CTPB content in the blend is increased.

FTIR spectrums of individual polymers of ECN and CTPB are shown in Figure 4. Neat epoxy shows peak at 910 and 860 $cm^{-1}$ due to oxirane functionality; those due to CTPB were obtained at 1700–1725 $cm^{-1}$ (carbonyl stretching of —COOH) and 1550–1610 $cm^{-1}$ (carboxylate anion stretching of —COOH). The disappearance of the peaks at 860, 910, 1310, 1350, 1700–1725, and 1825 $cm^{-1}$ and a simultaneous appearance of a new stretched peak at 1300–1400 $cm^{-1}$ of the carboxylate anion in the blends show the epoxy–CTPB reaction. However, an insufficient rubber content (e.g., at 5 wt %, the epoxy group is not completely consumed by —COOH) leads to the occurrence of both carboxylate and oxirane peaks in the infrared spectra for this blend. Similarly, at 25 wt % rubber concentration, although the epoxy group disappears completely, unreacted —COOH shows its presence, along with the ester crosslinks.

Flexural testing of blends were conducted as per ASTM method no. 1842 at room temperature (25 ± 2°C) on the Universal Testing Machine

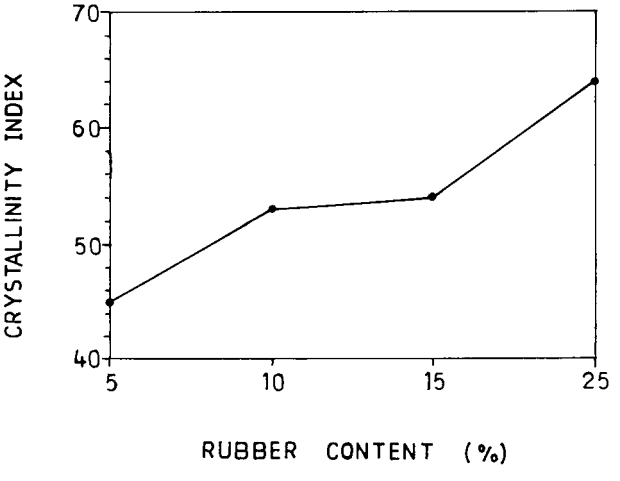


**Figure 3** CI of the blends.

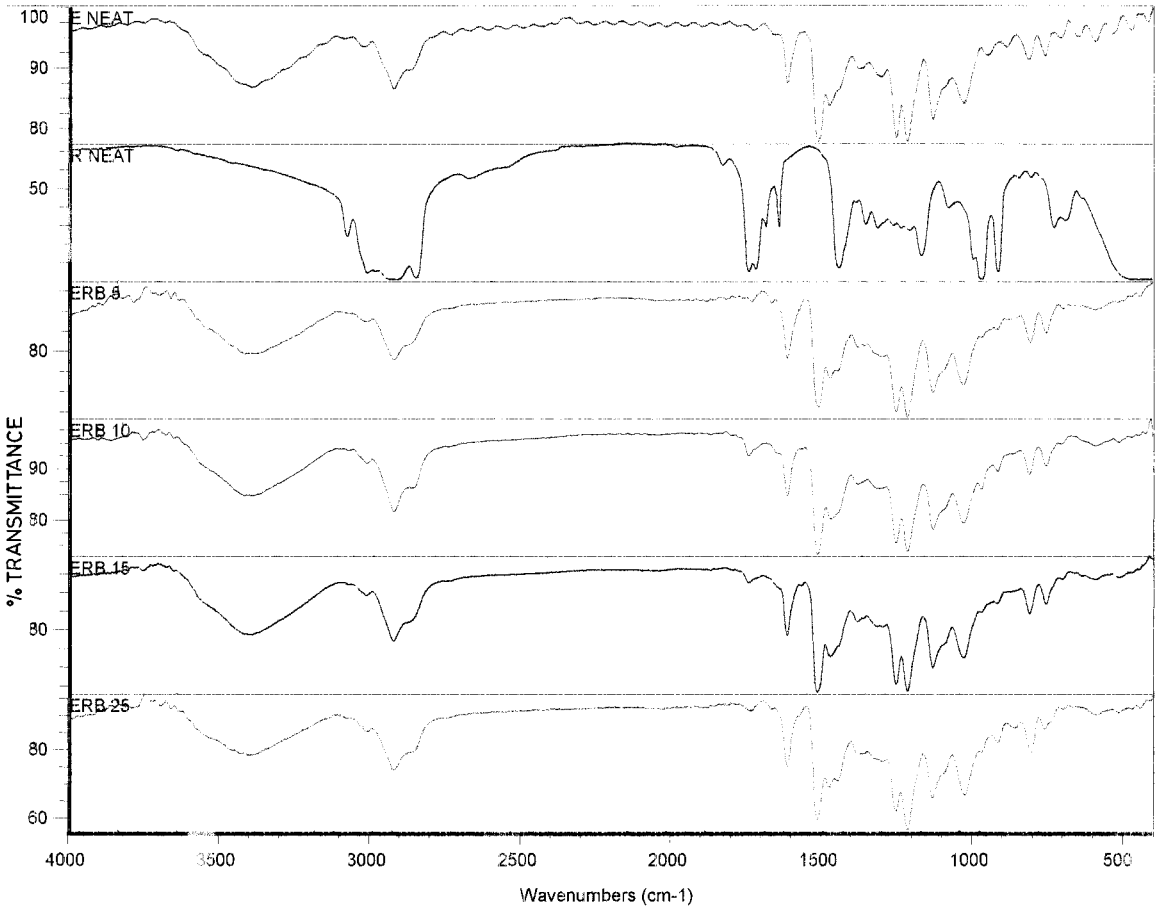


**Figure 4** FTIR spectrums of ECN, CTPB, and different epoxy–rubber blends.

(Tinius Olsen model) at $\frac{1}{8}$ in. $min^{-1}$, speed and the properties are appended in Table IV. SEM photomicrographs of flex-failed surfaces revealed that the basic mechanism of shear deformation and crazing persists, and relative proximity of one to the other is, however, controlled by the amount of rubber content present in the blend. Phase morphology of flex-fractured samples of epoxy neat (Fig. 5), as well as blend with 5 wt % CTPB

**Table IV Flexural Properties of ECN–CTPB Blend Castings**

| Blend No.[a] | Flexural Strength (MPa) | Flexural Modulus (GPa) |
|---|---|---|
| $ERB_0$ | 32.76 | 1.68 |
| $ERB_5$ | 34.87 | 1.71 |
| $ERB_{10}$ | 38.25 | 1.73 |
| $ERB_{15}$ | 16.90 | 1.23 |
| $ERB_{25}$ | 14.32 | 1.10 |

[a] ERB indicates epoxy–rubber blend; subscript indicates percent of rubber content.

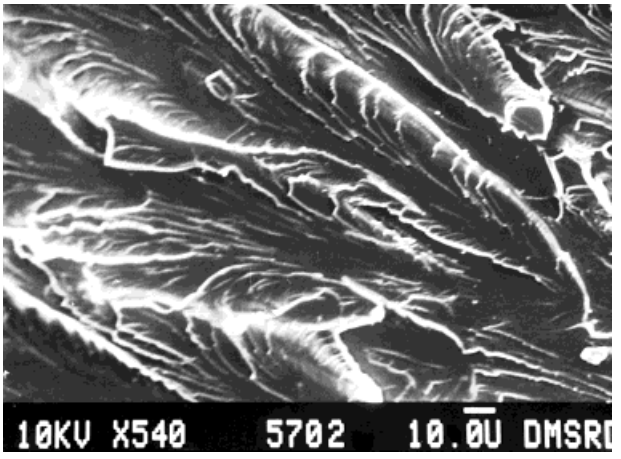


**Figure 5** SEM photomicrograph of flex-fractured surface of neat epoxy.

show a paraboloid or clam-shaped fracture indicating brittle failure. However, increased CTPB concentration (e.g., at the 10 wt % level) showed discrete two-phase morphology consisting of dispersed rubber particles (average size: 10 $\mu$m) uniformly dispersed in the continuous epoxy matrix (Fig. 6). Propagation of multiple fracture fronts in the form of steady tear lines, as well as hinderance offered by the rubber particles on the path of fracture propagation, are also evident. Rubber particles in this case act as stress raisers and consequently resulted in improved flexural properties of these blends. A smart fall in the flexural strength, as well as the flexural modulus, occurred when rubber concentration exceeds 10 parts. In this case, blends with higher rubber content showed epoxy occlusions inside the rubber particles, as well as substantial growth of the rubber phase. Absence of any smooth tear lines or deviation of fracture propagation are not visible (Fig. 7). This leads to a substantial fall in both flexural strength and flexural modulus for these blends. The WAXS studies and the absolute values of $\langle R \rangle$ and $\langle HW \rangle$ as described in Table IV also corroborate SEM observations.

## CONCLUSIONS

1. The combination of X-ray and FTIR techniques have been demonstrated to be accurate and reliable methods for characterization of toughened epoxy, as well as understanding the mechanism of toughening.
2. 10 wt % of CTPB into the epoxy network has been found to be the optimum concentration for toughening.
3. SEM studies on phase morphology closely resemble WAXS observations, as well as provide insight into the failure mechanism.

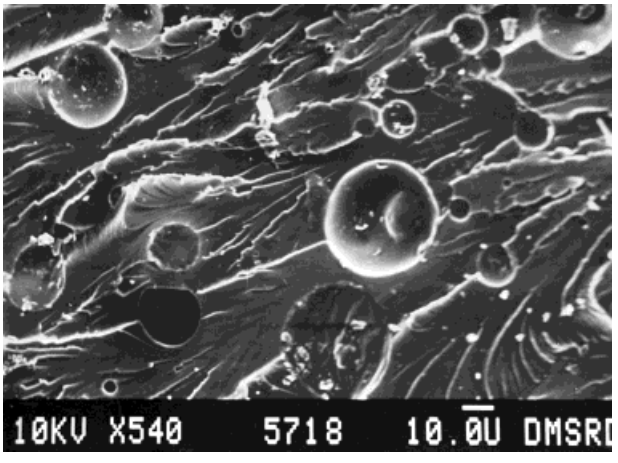


**Figure 6** SEM photomicrograph of flex-fractured surface of the blend with 10 wt % rubber.

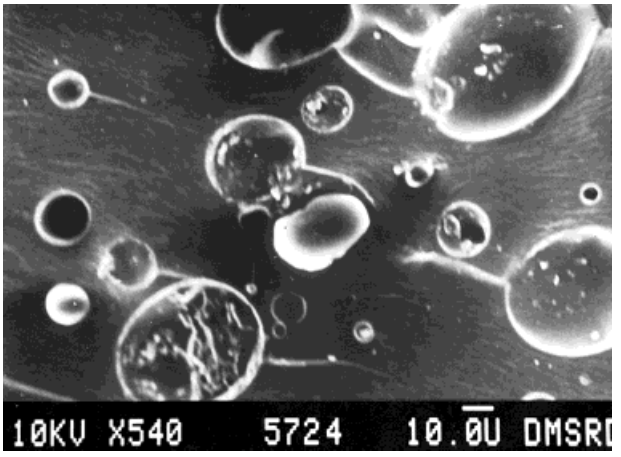


**Figure 7** SEM photomicrograph of flex-fractured surface of the blend with 25 wt % rubber.

## REFERENCES

1. A. J. Kinloch, in *Rubber-toughened Plastics,* C. K. Riew, Ed. (*Advances in Chemistry Series 22*), American Chemical Society, Washington, DC, 1989, p. 67.
2. A. J. Kinloch, S. J. Shaw, and D. L. Hunston, *Polymer,* **24,** 1355 (1983).
3. A. F. Yee and R. A. Pearson, *J. Mater. Sci.,* **21,** 2462 (1986).
4. R. A. Pearson and A. F. Yee, *J. Mater. Sci.,* **21,** 2475 (1986).
5. J. Huang and A. J. Kinloch, *J. Mater. Sci.,* **27,** 2753 (1992).
6. J. Huang and A. J. Kinloch, *J. Mater. Sci.,* **27,** 2763 (1992).
7. J. Huang and A. J. Kinloch, *J. Mater. Sci.,* **33,** 1330 (1992).
8. F. J. Guild and A. J. Kinloch, *J. Mater. Sci.,* **30,** 1689 (1995).
9. J. N. Sultan, R. C. Liable, and F. J. McGarry, *Polym. Symp.,* **16,** 127 (1971).
10. J. N. Sultan and F. J. McGarry, *Polym. Eng. Sci.,* **13,** 29 (1973).
11. W. D. Bascom, R. L. Cottington, R. L. Jones, and P. Peyser, *J. Appl. Polym. Sci.,* **19,** 2425 (1975).
12. R. J. Riew, E. H. Rowe, and A. R. Siebert, *ACS Adv. Chem. Ser.,* **154,** 326 (1976).
13. S. Kunz-Douglass, P. W. R. Beaumont, and M. F. Ashby, *J. Mater. Sci.,* **15,** 1109 (1980).

14. J. A. Sayer, S. C. Kunz, and R. A. Assink, *ACS Div. Polym. Mater. Sci. Eng.,* **49,** 442 (1983).
15. A. J. Kinloch, S. J. Shaw, D. A. Tod, and D. L. Hunston, *Polymer,* **24,** 1355 (1983).
16. C. B. Bucknall, *Toughened Plastics,* Applied Science Publishers, London, 1977.
17. P. Newman and S. Newman, *Polymer Blends,* Vols. 1 and 2, Academic Press, New York, 1978.
18. R. A. Pearson and A. F. Yee, *J. Mater. Sci.,* **24,** 2571 (1989).
19. R. A. Pearson and A. F. Yee, *J. Mater. Sci.,* **26,** 3828 (1971).
20. N. K. Kalfoglou and H. L. Williams, *J. Appl. Polym. Sci.,* **17,** 1377 (1973).
21. J. Y. Qian, R. A. Pearson, V. L. Dimonie, and M. S. El. Aasser, *J. Appl. Polym. Sci.,* **58,** 439 (1995).
22. R. Bagheri and R. A. Pearson, *J. Appl. Polym. Sci.,* **58,** 427 (1995).
23. T. K. Chen and Y. H. Jan, *Polym. Eng. Sci.,* **35,** 778 (1995).
24. A. J. Kinloch and D. L. Hunston, *J. Mater. Sci.,* **6,** 131 (1987).
25. V. Nigam, M. N. Saraf, and G. N. Mathur, *J. Thermal Anal.,* **49,** 483 (1997).
26. V. Nigam, M. N. Saraf, D. K. Setua, and G. N. Mathur, International Rubber Conference, Calcutta, December 12–14, Vol. 1, 1997, p. 57.
27. A. F. Halasa, G. D. Wathen, W. L. Hsu, B. A. Matrana, and J. M. Massie, *J. Appl. Polym. Sci.,* **43,** 183 (1991).
28. S. C. Kunz, J. A. Sayre, and R. A. Assink, *Polymer,* **23,** 1877 (1983).
29. T. T. Wang and H. M. Zupko, *J. Appl. Polym. Sci.,* **26,** 2391 (1981).
30. J. K. Gillham and L. C. Chan, *Organ. Coat. Plast. Chem.,* **48,** 571 (1983).
31. D. Verchere, J. P. Pascault, H. Sautereau, S. M. Moschiar, C. C. Riccardi, and R. J. J. Williams, *J. Appl. Polym. Sci.,* **42,** 701 (1991).
32. S. M. Moschiar, C. C. Riccardi, R. J. J. Williams, D. Verchere, H. Sautereau, and J. P. Pascault, *J. Appl. Polym. Sci.,* **42,** 717 (1991).
33. R. Bagheri and R. A. Pearson, *J. Mater. Sci.,* **31,** 3945 (1996).
34. D. S. Kim, K. Cho, J. K. Kim, and C. E. Park, *Polym. Eng. Sci.,* **36,** 755 (1996).
35. D. K. Setua, S. K. Chakravorty, S. K. De, and B. K. Dhindaw, *J. Scan. Elect. Micros.,* **Part III,** 973 (1982).